Available online at www.sciencedirect.com
SCIENCE DIRECT®
Journal of Nuclear Materials 325 (2004) 94–106
journal of nuclear materials
www.elsevier.com/locate/jnucmat

The effect of oversized solute additions on the microstructure of 316SS irradiated with 5 MeV Ni^{++} ions or 3.2 MeV protons

J. Gan [a,*], E.P. Simonen [b], S.M. Bruemmer [b], L. Fournier [c], B.H. Sencer [c], G.S. Was [c]

[a] *Argonne National Laboratory-West, Nuclear Technology Division, P.O. Box 2528, Idaho Falls, ID 83403, USA*
[b] *Pacific Northwest National Laboratory, Richland, WA 99352, USA*
[c] *The University of Michigan, Ann Arbor, MI 48109, USA*

Received 6 June 2002; accepted 11 November 2003

Abstract

The effect of the oversized hafnium or platinum (0.3 at.%) solutes on the evolution of irradiated microstructure in 316SS was investigated. Irradiations were conducted with 5 MeV Ni-ions at 500 °C to doses up to 50 dpa or with 3.2 MeV protons at 400 °C to a dose of 2.5 dpa, and previous studies demonstrated that these irradiations are capable of producing similar irradiated microstructure and microchemistry relevant to LWR cores. Microstructures of 316SS, 316SS + 0.3 at.% Pt and 316SS + 0.3 at.% Hf were characterized using transmission electron microscopy. The addition of Hf showed a strong effect in suppressing radiation-induced microstructure evolution; no voids were observed at doses up to 50 dpa for Ni-ion irradiation and 2.5 dpa for proton irradiation. The mean diameter of the Frank loops in the Hf-doped samples is about 40% smaller than loops in 316SS. The microstructural examinations from both types of particle irradiation revealed that for 0.3 at.% Pt addition there is no beneficial effect on irradiated microstructure. The mechanisms for the role of oversize solute additions on the microstructure evolution are discussed.

1. Introduction

The objective of this work is to develop the scientific basis for a new class of radiation-resistant materials to meet the needs for higher performance and extended life in next generation power reactors. New structural materials are being designed to delay or eliminate the detrimental radiation-induced changes that occur in austenitic alloys, i.e., a significant increase in strength and loss in ductility, environment-induced cracking, swelling and embrittlement. A mechanistic approach is taken to ameliorate the root causes of materials degradation in current light water reactor (LWR) and next generation reactor systems. The effective improvements in materials design are best based on mechanistic understanding of radiation damage processes and environmental degradation. This work used solute atom addition of Pt or Hf in 316SS. Platinum addition in 316SS was beneficial in improving the resistance to stress corrosion cracking [1], however its effect on the irradiated microstructure has never been investigated. Hf addition in 316SS has been investigated for neutron and electron irradiation [2–4], however, the irradiation conditions were irrelevant to LWR cores and the dose dependence of the irradiated microstructure has not been established. The calculated linear size factors for various oversized elements used in this work and other works are listed in Table 1. Pt has smaller size misfit while Hf has large size misfit although both have about equal atomic mass.

* Corresponding author.
E-mail address: jian.gan@anl.gov (J. Gan).

0022-3115/$ - see front matter © 2003 Elsevier B.V. All rights reserved.
doi:10.1016/j.jnucmat.2003.11.002

Table 1
Physical properties for various oversized solute atoms

Element	316SS	Pt	Ti	Nb	Hf	Zr
Atomic number	N/A	78	22	41	72	40
Atomic mass (g)	55	195.08	47.88	92.91	178.46	91.23
Density (g/cm^3)	7.89	21.45	4.51	8.58	13.31	6.51
Atomic volume (cm^3/mol)	6.86	9.09	10.62	10.83	13.41	14.01
Linear size factor (%)	0	**9.84**	15.68	16.44	**25.04**	26.87

Note: Linear size factor is calculated as: $L_{sf} = \{(\Omega_{add}/\Omega_{sol})^{1/3} - 1\} \times 100(\%)$ where Ω_{sol} and Ω_{add} is the atomic volume of the solvent and the additive, respectively.

The effect of misfit elements on the irradiated microstructure and microchemistry have been investigated by several workers. The early work by Smidt and Sprague investigated the suppression of void nucleation by a vacancy trapping mechanism [5]. Iron-based binary alloys with 0.3 at.% solute addition (Cu, Ni, V, P) were used and irradiated with neutrons in the EBR-II at 525 °C to a fluence of 8.5×10^{21} n/cm^2 ($E > 0.1$ MeV). Voids were observed in all alloys except the Fe–0.3at.%V. It was believed that the oversized solute addition suppressed voids by vacancy trapping at solute atoms, thus reducing the free vacancy concentration in the matrix [6]. The work by Wilsdorf [7] on the suppression of void nucleation by oversized solute addition suggested that the interaction between vacancies and internal stress fields is a more favorable mechanism. A comprehensive review by Garner [8] on the effect of solute addition on void swelling discussed the effect of small amounts of solute addition in 316SS on void swelling. The studies on the solute addition of Ti, Si, Zr, Cr, Mo, C and P at different concentration levels in neutron-irradiated 316SS indicated that their influence was only on the duration of the transition regime for void swelling. It was pointed out that for solution annealed AISI 316SS, carbon in solution might suppress voids at low temperature but promotes swelling at high temperature.

Kato et al. [2,3] investigated void formation and radiation-induced segregation (RIS) in electron-irradiated 316L SS modified by addition of 0.35 at.% of V, Ti, Nb, Ta, Zr and Hf. Void formation in the matrix at 500 °C was reduced significantly by the added oversize solutes and Hf appeared to be the most effective solute addition by showing no voids at a dose of 10.8 dpa. The Hf solute addition was also very effective in suppressing RIS evidenced by nearly no Cr-depletion at a dose of 10.8 dpa (500 °C). It was concluded that the effect of the oversized solute addition on RIS was due to an enhanced recombination and a reduction of mobility of point defects in the matrix caused by point defect trapping at oversized atoms (vacancy binding with oversized atoms). The same alloys, 316L + 0.35 at.% of V, Ti, Nb, Ta, Zr or Hf were also irradiated with fast neutrons in the Fast Flux Test Facility (FFTF) to a dose of about 32 dpa at temperatures of 425, 520 and 600 °C [4]. Considering the relevance to an LWR core, the results for 425 °C showed voids and dislocation structure (loop data not provided). It was concluded that the Zr and Hf additions were the most effective solutes for suppressing swelling compared to other solutes examined for neutron irradiation.

The concept of using oversized solutes to affect defect migration and aggregation is being re-explored for the development of advanced materials for the next generation nuclear power systems. It is anticipated that the next generation of advanced nuclear power systems will operate at higher temperatures and higher thermal neutron fluxes than the existing LWR systems. Our work focused on understanding at LWR-relevant temperatures. This work used Ni-ion and proton irradiation to study the effects of misfit elements, Hf and Pt, on the radiation-induced microstructure in alloys 316SS. Heavy-ion and proton irradiations are used due to the advantages that previous experience demonstrated that these irradiations could effectively produce similar radiation-induced microstructure and microchemistry relevant to LWRs at around 300 °C [9–14]. The use of heavy-ion and proton irradiation in this work also distinguishes whether the major effect of the solute additions is on cascade processes or isolated point defect kinetics during the development of irradiated microstructure. It is well known that the cascade morphology between the two types of irradiation is very different. If the effect of solute additions is mainly during the cascade phase, then heavy-ion irradiation should show a much stronger effect than proton irradiation.

This is the first investigation on the effect of Pt as a solute addition on irradiated microstructure due to its inert chemical stability in contrast to the reactive element Hf. It is expected that Pt addition may have little or no effect on the matrix chemistry. Since Hf has a large size misfit factor than Pt, if the effect of size misfit on microstructure is significant, then Hf addition should show a much stronger effect than Pt addition. Through comparisons of the oversized solute effects on irradiated microstructure from both heavy-ion and proton irradiations, mechanisms can be delineated based on in-cascade processes or post-cascade processes.

2. Experiments

Three high-purity austenitic stainless steel alloys supplied by General Electric Corporate Research & Development were used in this study. The alloys consisted of a 316L SS and two alloys with the same composition but doped with 0.3 at.% Pt (316SS + Pt) or 0.3 at.% Hf (316SS + Hf). The compositions of these three alloys are given in Table 2. As-received alloys were solution annealed at 1200 °C for 1 h and water quenched prior to 70% cold working. Cold working was followed by annealing at 900 °C for 20 min and water quenching to obtain a grain size of about 10 μm. Hafnium-rich precipitates with a density of 8.6×10^{20} m^{-3} and a mean size of 25 nm were observed in the 316SS + Hf alloy annealed at 900 °C for 20 min [15]. In addition to the heat treatment at 900 °C for 20 min, the alloy 316 + Hf was also heat treated at 1100 °C for 30 min to put additional Hf back in solution. This heat treatment resulted in a grain size of about 20 μm, a decrease in the Hf-rich precipitate density to 1×10^{19} m^{-3} as well as an increase in mean size to 129 nm. The 1100 °C heat treatment temperature was chosen based on a balance between increased grain size and reduced precipitate microstructure.

Photomicrographs of grain structures using scanning electron microscopy (SEM) and defect microstructures using transmission electron microscopy (TEM) for the non-irradiated material conditions are shown in Fig. 1. For the same heat treatment, the Pt-doped alloy has grain sizes smaller than the base alloy and the Hf-doped alloy has the smallest grain sizes. A low density of network dislocations is observed with precipitates in the Hf-doped alloys. Prior to Ni-ion irradiation the samples were wet-polished with SiC paper to 600-grit, diamond abrasive film to 3-μm and a final polish with 0.3-μm alumina. For the proton irradiation, the specimens were polished to a 4000-grit SiC paper finish and then electropolished in a 60% phosphoric acid and 40% sulfuric acid solution at 45 °C for 3 min at 30 V.

Nickel-ion irradiation was conducted using an ion accelerator with a 3.4 MV terminal voltage at the Pacific Northwest National Laboratory. The sample temperature was held at 500 °C and monitored using a thermocouple and an optical pyrometer. Calibration experiments were performed to ensure a temperature within ±10 °C of the planned irradiation. During irradiation, typical pressures in the target chamber were in the low-to-mid 10^{-8} Torr range. The 5 MeV Ni^{++} ions are used at a current density of 90 nA on an irradiated area of 7×7 mm^2. Using the TRIM 2000 code, the calculated displacement rate is 4.73×10^{-4} dpa/s at a depth of 0.5 μm. The dpa calculations are based on a displacement energy of 40 eV and an alloy composition

Table 2
Nominal composition of the alloys used in this work (at.%)

Alloy	Fe	Cr	Ni	Mn	Mo	Si	C	Solute addition
316SS	Bal.	18.6	13.3	1.2	1.3	0.16	0.09	None
316L + Pt	Bal.	18.7	13.4	1.2	1.3	0.16	0.09	0.3 at.% Pt
316L + Hf	Bal.	18.7	13.4	1.2	1.3	0.16	0.09	0.3 at.% Hf

Note that the atomic fraction of the addition of Pt or Hf in 316SS is 0.3 at.%.

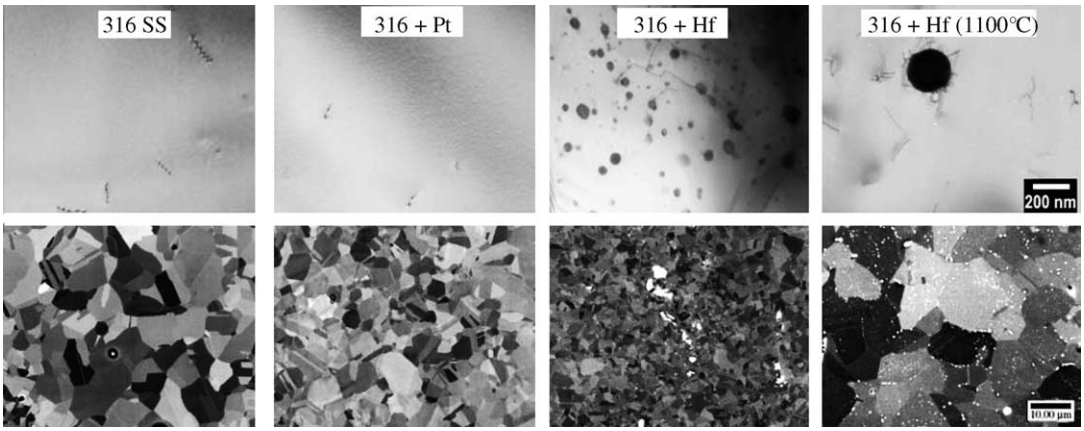

Fig. 1. Micrographs show material condition prior to irradiation after heat treatment at 900 °C other than specified. A low density of network dislocations is observed with precipitates only in the Hf-doped alloys. The marker is 200 nm for TEM pictures of microstructure (top) and 10 μm for SEM pictures of grain structure (bottom).

for 316SS. Proton irradiations were conducted at 400 °C with 3.2 MeV protons at the Michigan Ion Beam Laboratory at the University of Michigan. The irradiation dose rate of approximately 8.5×10^{-6} dpa/s was used, resulting in a nearly uniform damaged layer throughout the first 35 μm of the proton range (~40 μm). Details of the irradiation technique have been previously described [16]. The temperatures for Ni-ion and proton irradiations were chosen to compensate for the damage rate difference in order to produce irradiation damage in materials relevant to LWR cores, demonstrated by the previous works [9–14].

For both Ni-ion irradiated specimens and proton-irradiated specimens, 3-mm TEM discs were prepared. Before back-thinning to perforation, a surface layer of 0.5 μm for Ni-ion irradiation and 10 μm for proton irradiation from the irradiated side was removed. Radiation-induced microstructures were characterized using TEM. Quantitative analyses of the irradiated microstructures were carried out and the dose dependence of densities and sizes for Frank loops, voids and precipitates were obtained. Rel-rod images of Frank loops [17] were used for loop measurements and bright-field images were used for voids and precipitate measurements.

3. Results

The microstructural characterization revealed that the irradiated microstructure mainly consisted of Frank loops and voids. The present research confirmed that a low concentration of large misfit atoms alters the microstructural evolution. Void formation and swelling was suppressed by the Hf addition for both charged particle irradiations, while the Pt addition had no beneficial effect. The results of Ni-ion irradiation and proton irradiation were in reasonable agreement despite the difference in cascade morphology and damage rate. Radiation-induced microstructure mainly consisted of Frank loops and voids with significant difference among the three alloys examined. In addition to density and size of the Frank loops and voids, the interstitial volume fraction and void swelling were calculated which indicate the inventory of interstitials and vacancies in the observed defect structures.

In the unirradiated condition, the base alloy and the Pt-doped alloy revealed a clean microstructure with a low density of line dislocations. In contrast, the Hf-doped alloy revealed a fine distribution of precipitates along with scattered large irregular inclusions, as presented in Fig. 1. The precipitates shown in TEM pictures were identified as $HfNi_5$ intermetallics and the large inclusions shown in SEM pictures were identified as HfC. It is expected that the Hf-rich phase precipitated during cooling from the solution annealing temperature and did not dissolve during the 900 °C heat treatment. A heat treatment at 1100 °C for 30 min substantially coarsened the $HfNi_5$ intermetallic particles and reduced their density by two orders of magnitude. It is believed that the 1100 °C heat treatment put more Hf back into solution.

3.1. 5 MeV Ni-ion irradiation at 500 °C

The three alloys were characterized at doses of 0.5, 2.0, 10, 30 and 50 dpa. The bright-field images of dislocation loop structure for alloys irradiated to doses of 0.5, 2.0, 10 and 50 dpa are shown in Fig. 2. The dislocation distributions are uniform at doses above 0.5 dpa. Accordingly, the rel-rod dark-field images of the Frank loops are shown in Fig. 3. Note that these pictures are taken from areas with different thickness and the number of loops in the pictures cannot be directly related to the measured loop density. One distinct feature is that loop sizes in the Hf-doped alloy are smaller than those in the 316SS and 316 + Pt alloys. Micrographs indicating the presence of voids at various doses for the three alloys are shown in Fig. 4. Void distributions were non-uniform particularly at low doses. Voids were completely suppressed in the alloy 316 + Hf (900 °C HT) up to a dose of 10 dpa and in the alloy 316 + Hf (1100 °C HT) where no voids were observed up to a dose of 50 dpa.

Measurements of densities and sizes of Frank loops, voids and precipitates after Ni-ion irradiation at 500 °C and proton irradiation at 400 °C are summarized in Table 3. The smaller loop sizes in the Hf-doped alloys are evident. Dose dependence of Frank loop densities is shown in Fig. 5. The loop densities as a function of dose in Hf-doped alloys appeared to be different from those in the base alloy and the Pt-doped alloy. Loop densities in Hf-doped alloys increase from a dose of 10–50 dpa, in contrast to the base alloy and the Pt-doped alloy where loop densities appeared to saturate between doses of 10 and 50 dpa.

Frank loop sizes as a function of dose are shown in Fig. 6. A distinct feature is the smaller loop sizes in both 316 + Hf conditions at all doses. Alloy 316 + Pt showed a large loop size at a dose of 2 dpa. It was noticed that the loop size distribution in the Hf-containing alloys is narrower than in the alloy 316SS and 316 + Pt. To investigate the interstitial partitioning, the inventory of interstitials in the Frank loops was estimated by calculating the loop volume fraction at various doses, shown in Fig. 7. The interstitial volume fraction is defined as the product of the Frank loop density, the average loop area and the thickness of the {1 1 1} plane (0.207 nm). The alloy 316 + Hf (1100 °C HT) has the lowest total amount of interstitials in the form of Frank loops at 10 dpa, but continue to increase with a trend different than alloys 316SS and 316 + Pt. The interstitial inventory in

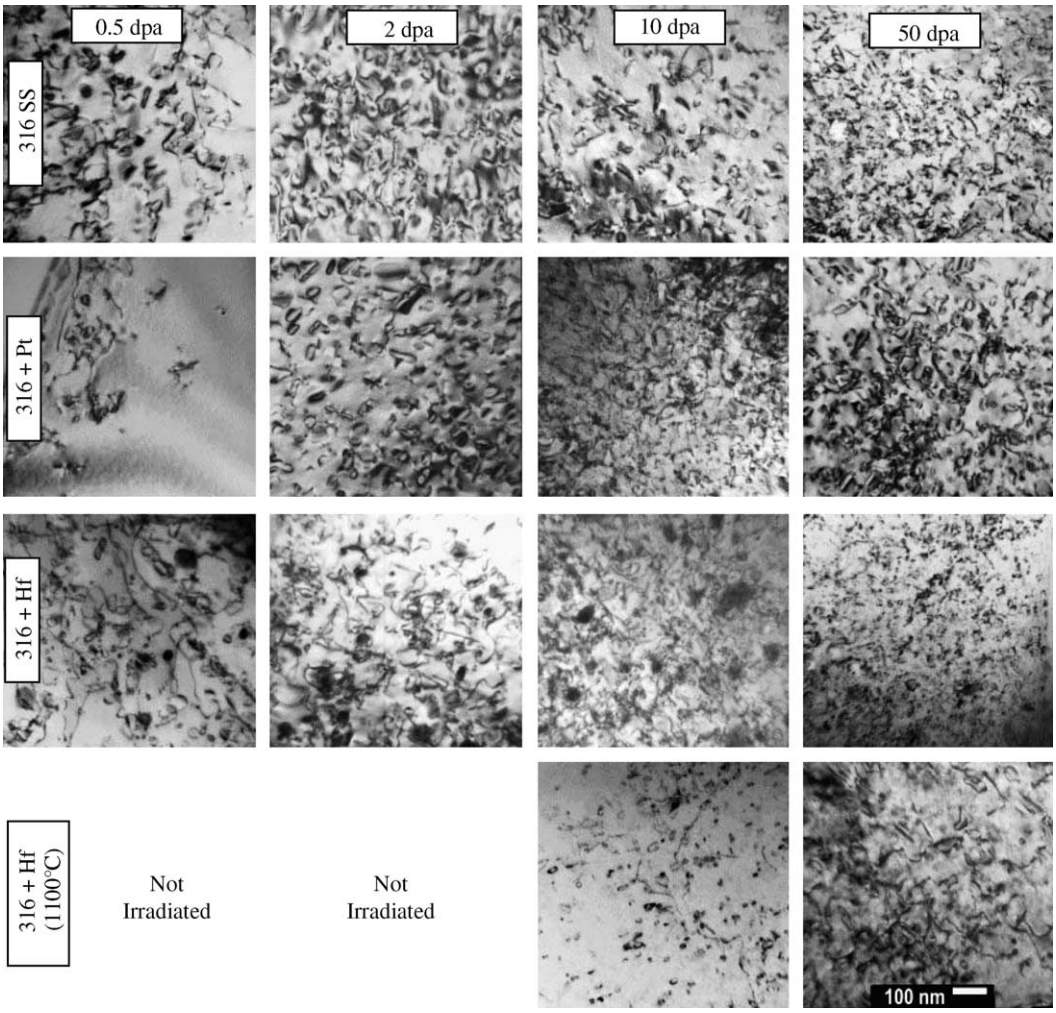

Fig. 2. Bright-field micrographs of loop images for the three alloys irradiated to the indicated dose. Both faulted and unfaulted loops are imaged. Note the very high density of dislocation line length compared to the non-irradiated case. Larger loops of irregular geometry are unfaulted loops. The very dense image makes loop characterization difficult using bright-field techniques. The marker in the inset indicates 100 nm.

the Frank loops is greater for alloy 316 + Pt at 2–10 dpa and for alloy 316 + Hf at 30 dpa and above.

The measured void number densities were very low, often non-uniform and difficult to characterize statistically. The base alloy revealed a low number density ($<10^{20}$ m^{-3}) of non-uniform voids up to 10 dpa but revealed a large number density ($\sim 2\times10^{20}$ m^{-3}) and size ($\sim$30 nm) at 50 dpa as seen in Figs. 8 and 9, respectively. The Pt-containing alloy revealed a slightly higher void number density and size than the base alloy. The alloy 316 + Hf (900 °C HT) showed delayed void swelling up to a dose of 10 dpa while the alloy 316 + Hf (1100 °C HT) completely suppressed the void swelling up to a dose of 50 dpa. Measured average void sizes in these alloys ranged from 18 nm to 33 nm as indicated in Table 3. Similar to loop sizes, it was noticed that void size distribution at a dose 50 dpa in 316 + Hf (900 °C HT) is narrower than in the other two alloys. The dose dependence of void swelling is shown in Fig. 10. Swelling is the highest in the alloy 316 + Pt for all the doses examined. Note that the swelling at 50 dpa for alloy 316SS, 316 + Pt and 316 + Hf (900 °C HT) are equivalent.

The Hf-doped alloys in the non-irradiated condition exhibited a distribution of $HfNi_5$ intermetallics precipitates along with large irregular-shaped HfC (>1 μm) scattered in the matrix, Fig. 1. The effect of increasing dose on number density and size of the $HfNi_5$ intermetallics is shown in Fig. 11 for the alloy 316 + Hf (900 °C HT). The number density decreases as

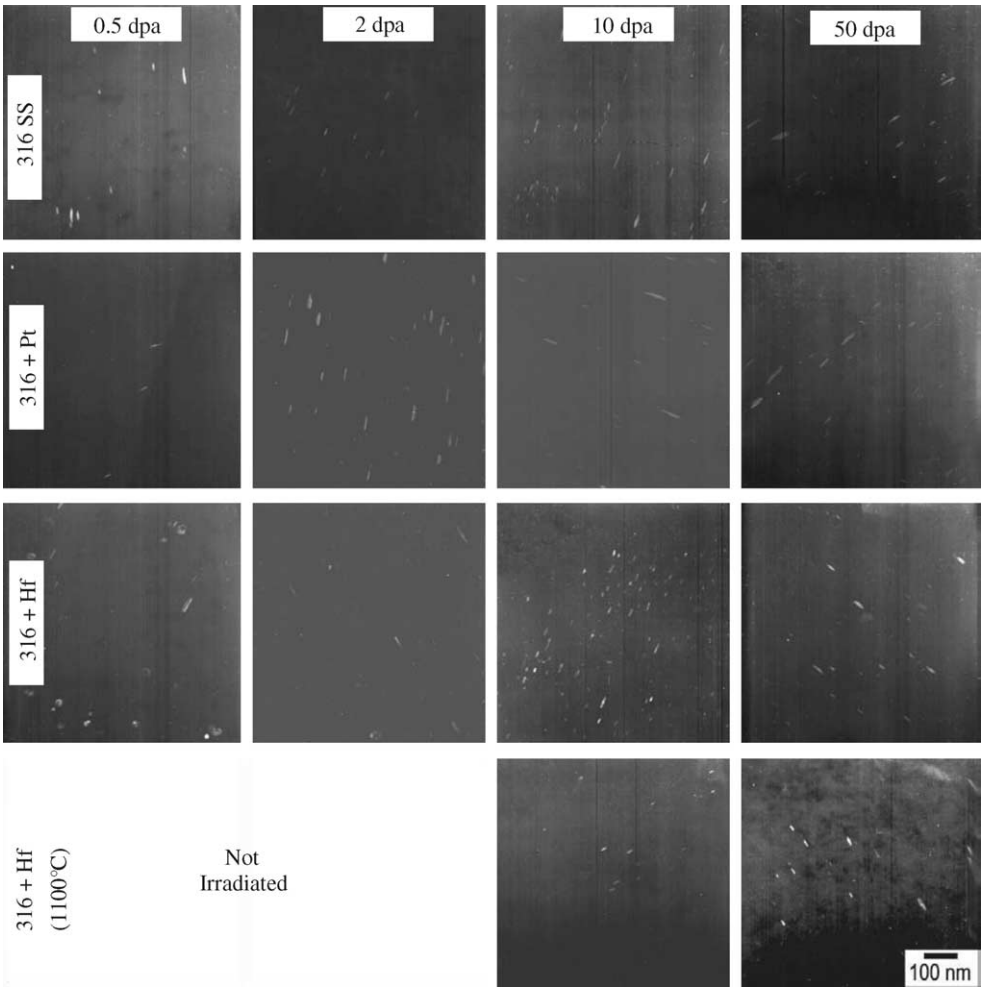

Fig. 3. Rel-rod micrographs of loop images for the three alloys irradiated to the indicated doses. The short line segments are loop images. The rel-rod technique only images faulted dislocation loops. Because of diffraction conditions, only 1/4 of the loops can be imaged for one specimen orientation. This technique provides better visibility for identifying individual loops. The marker in the inset indicates 50 nm.

the size increases up to a dose of 30 dpa and then stabilizes between 30 and 50 dpa. The estimated Hf inventories in the HfNi5 intermetallic particles for 316 + Hf (900 °C HT) were 0.13 at.% at doses of 0.5–2.0 dpa, 0.1 at.% at 10 dpa and about 0.06 at.% at 30–50 dpa. Note that the $HfNi_5$ intermetallic density in the alloy 316 + Hf (1100 °C HT) is below $10^{19}/m^3$, about 100 times lower than in 900 °C heat-treated material, thus an estimation of Hf inventory was not available for this alloy.

3.2. MeV proton irradiation at 400 °C

The effect of oversized solute additions (0.3 at.% Pt, 0.3 at.% Hf) on the irradiated microstructure was also investigated using proton irradiation at 400 °C to a dose of 2.5 dpa. For the 316 + Hf alloy, only the 1100 °C condition was used. The results from proton irradiation are in agreement with Ni-ion irradiation at 500 °C to doses of 2 and 10 dpa as indicated in Table 3. The 316 + Pt alloy has a larger loop size, void density and void size in comparison to the base alloy. The 316 + Hf alloy has a smaller loop size and no voids compared to the base alloy. Micrographs of loops and voids in the 316 + Pt alloy after Ni-ion irradiation to doses of 2 and 10 dpa and proton irradiation to a dose of 2.5 dpa are shown in Fig. 12. The comparison of the results between Ni-ion and proton irradiation is shown in Fig. 13(a)–(e). Ni-ion and proton irradiations reveal similar microstructural responses with oversized solute addition with an exception that the void number density in the proton-irradiated 316 + Pt alloy at a dose of 2.5 dpa is

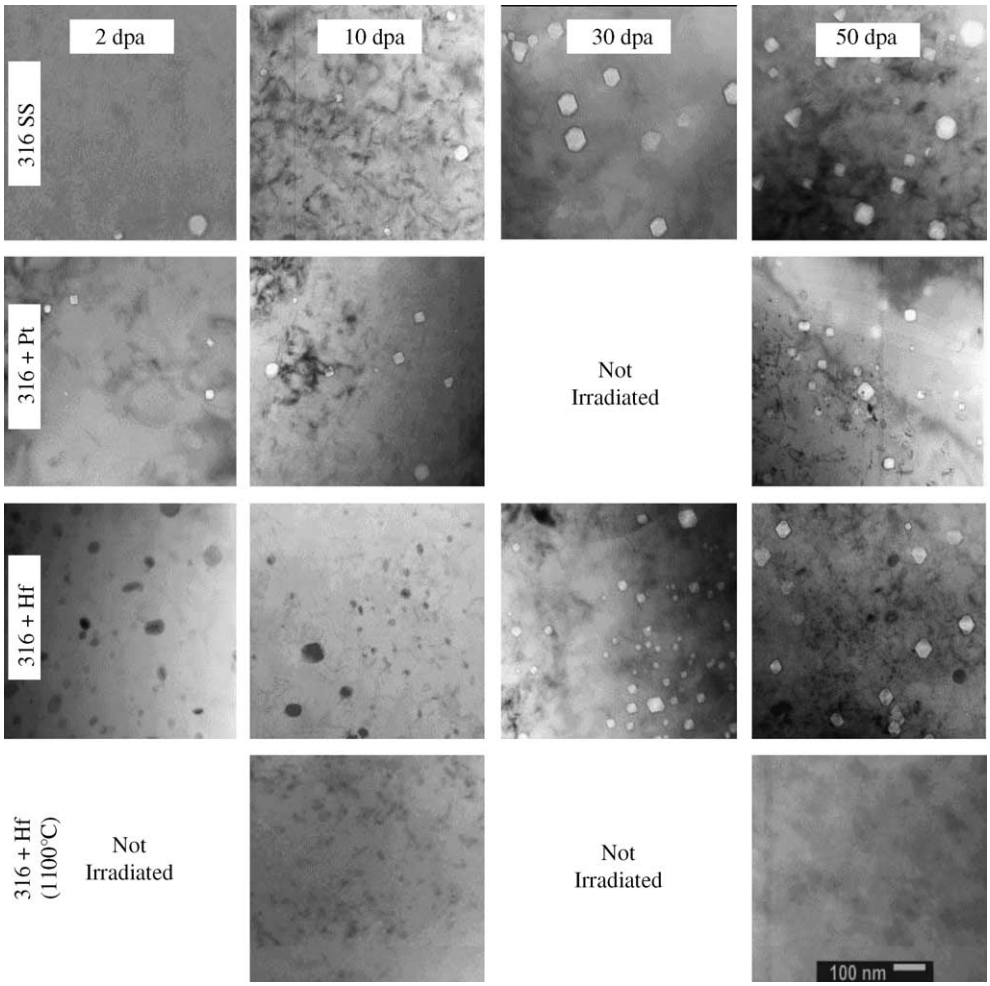

Fig. 4. Micrographs of voids for the three alloys irradiated to the indicated doses. Voids are only predominant at 50 dpa. The density was marginally high enough to obtain an estimate at 10 dpa. For the Pt- and Hf-containing alloys, the images shown represent local areas of higher void density. Typically, a significant fraction of the areas examined showed no voids. The base alloy exhibited a uniform void distribution represented in the figure. The marker in the inset indicates 100 nm.

about 5 times higher than for Ni-ion irradiation at 2 dpa.

To summarize the results for microstructure measurements, the evolution of Frank loop structure in the Hf-doped alloys is different from the base alloy and the Pt-doped alloy. Loop density in the Hf-doped alloys continually increases with dose up to 50 dpa, with a smaller loop size than in the other two alloys. Void swelling is slightly higher in the Pt-doped alloy than in the base alloy. The alloy 316 + Hf (900 °C HT) exhibited a delayed void development up to a dose of 10 dpa and the alloy 316 + Hf (1100 °C HT) completely suppressed void formation to a dose of 50 dpa. Both Ni-ion and proton irradiations produce similar results on the alloy influence on irradiated microstructures such as higher swelling in alloy 316 + Pt and smaller loop sizes and no voids in the alloy 316 + Hf (1100 °C HT).

4. Discussion

The addition of oversized solute to 316SS can affect the material response to the irradiation in various ways. The comparisons of behavior in alloys containing Pt or Hf addition irradiated with Ni-ions and protons help to understand the mechanism which is important for the development of damage-resistant alloys. Key findings from the present microstructural analysis include (1) the significant improvement in void swelling for the 316 + Hf (1100 °C) alloy and (2) no beneficial effect for Pt addition on radiation-induced microstructure and (3)

Table 3
Microstructure measurements for alloys 316SS, 316 + Pt and 316 + Hf and 316 + Hf (optimized) irradiated with 5 MeV Ni^{++} ions at 500 °C or 3.2 MeV protons at 400 °C to various doses

	Irradiation type						
	Ni^{++} Ions						Proton
Dose, dpa	0	0.5	2.0	10	30	50	2.5
Loop density ($10^{20}/m^3$)							
316SS	0	4.3	9.4	6.9	7.4	8.8	9.5
316 + Pt	0	2.9	15	11	–	11	12
316 + Hf (900 °C)	0	6.0	9.6	23	45	58	–
316 + Hf (1100 °C)	0	–	–	8.2	–	19	31
Loop diameter (nm)							
316SS	0	22	24	25	25	25	30
316 + Pt	0	22	32	28	–	20	38
316 + Hf (900 °C)	0	17	15	14	13	13	–
316 + Hf (1100 °C)	0	–	–	14	–	16	13
Loop volume fraction (10^{-5})							
316SS	0	4.5	10	9.2	11	11	–
316 + Pt	0	2.7	29	17	–	9.3	–
316 + Hf (900 °C)	0	3.5	5.7	8.9	15	19	–
316 + Hf (1100 °C)	0	–	–	3.3	–	8.7	–
Void density ($10^{20}/m^3$)							
316SS	0	0	<0.21	0.43	0.80	2.1	1.0
316 + Pt	0	0	<0.28	0.62	–	2.7	4.0
316 + Hf (900 °C)	0	0	0	0	1.2	2.5	–
316 + Hf (1100 °C)	0	–	–	0	–	0	0
Void diameter (nm)							
316SS	0	0	18	21	33	27	13
316 + Pt	0	0	26	27	–	30	18
316 + Hf (900 °C)	0	0	0	0	25	29	–
316 + Hf (1100 °C)	0	–	–	0	–	0	0
Void swelling (%)							
316SS	0	0	0.01	0.03	0.26	0.46	0.03
316 + Pt	0	0	0.03	0.09	–	0.65	0.13
316 + Hf (900 °C)	0	0	0	0	0.15	0.45	–
316 + Hf (1100 °C)	0	–	–	0	–	0	0
Precipitate density ($10^{20}/m^3$)							
316 + Hf (900 °C)	6.5	8.6	8.6	6.0	2.0	1.9	–
316 + Hf (1100 °C)	0.096	–	–	0.040	–	0.085	–
Precipitate diameter (nm)							
316 + Hf (900 °C)	20	22	20	22	26	26	–
316 + Hf (1100 °C)	129	–	–	111	–	105	–

Note: The symbol (–) indicates no irradiation or measurement conducted.

consistent results between Ni-ion and proton irradiation.

Fundamentally, radiation effects are dominated by the production, recombination and annihilation of vacancies and interstitials. The mechanistic influence of oversized solute can be understood in terms of in-cascade recombination, intra-cascade recombination and partitioning of defects into accumulating microstructure and microchemistry. The roles of these mechanisms are considered in the following discussion to understand the observed effects.

4.1. Influence of Pt

Platinum is an inert element and no precipitates were identified in alloy 316 + Pt. The size misfit for Pt is not as big as the other oversized solutes as listed in Table 1. The Pt addition showed an adverse effect on

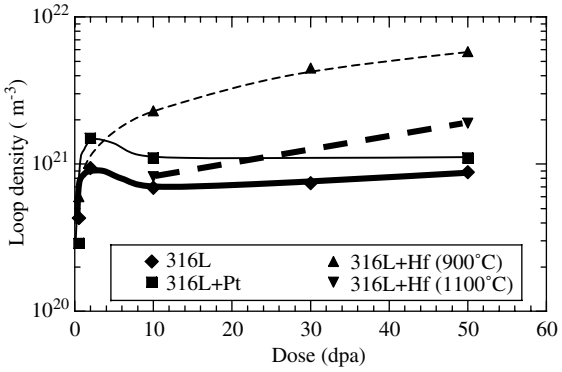

Fig. 5. Loop number density as a function of dose for the three alloys. The loop number densities in Hf-doped alloys did not saturate even at does up to 50 dpa. From 10 to 50 dpa loop density is the highest in 316 + Hf (900 °C).

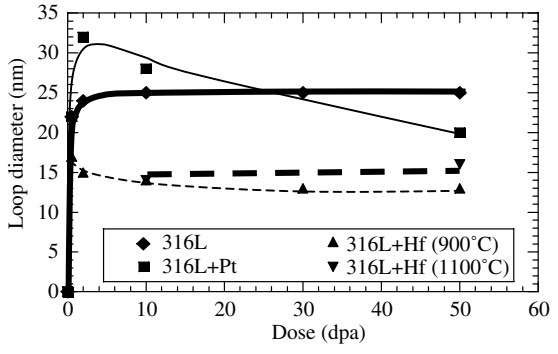

Fig. 6. Loop size as a function of dose for the three alloys. The loop sizes in Hf-doped alloys are smaller than in alloys of 316SS and 316 + Pt for all the doses.

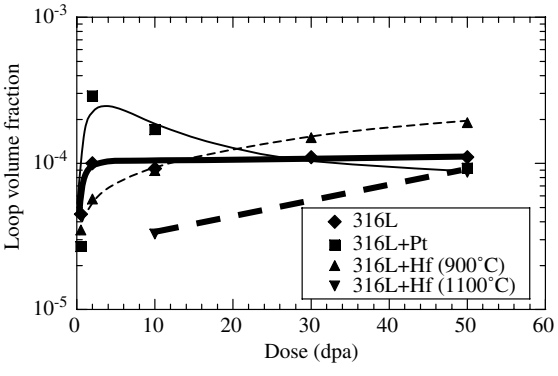

Fig. 7. The loop volume fraction is shown as a function of dose for the three alloys. The capacity to store interstitials in loops passes through a strong transient between 0 and 10 dpa for the alloys with Pt but not for the base alloy or the Hf-doped alloys.

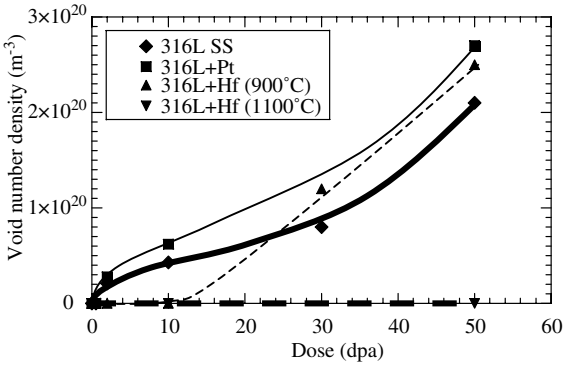

Fig. 8. Measured void number density as a function of dose. The base alloy exhibits a less void number density at 50 dpa compared to the alloys with Pt or Hf addition. The alloy 316 + Hf (1100 °C) exhibited no voids (thick dashed line).

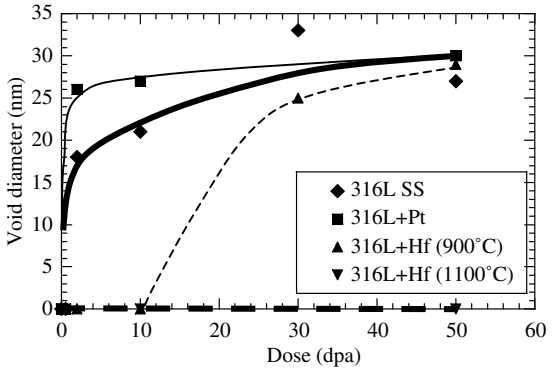

Fig. 9. Void size as a function of dose for Ni-ion irradiated alloys 316SS, 316 + Pt, 316 + Hf (900 °C) and 316 + Hf (1100 °C).

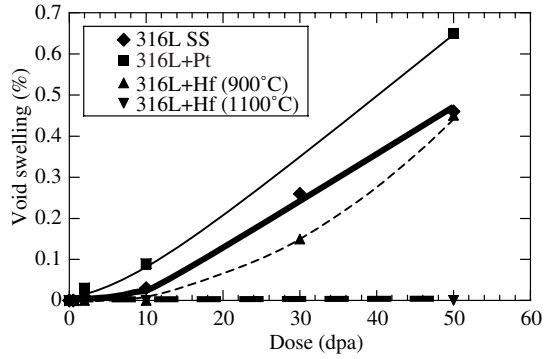

Fig. 10. Measured void volume fraction (swelling) is shown as a function of dose. Note that no voids were observed in alloy 316 + Hf (1100 °C) at a dose of 50 dpa.

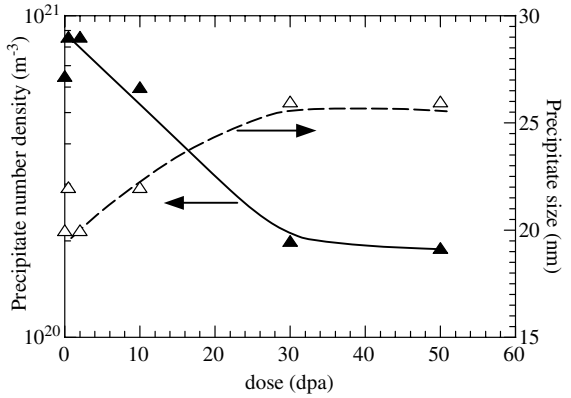

Fig. 11. Measured size and number density of Hf-containing precipitates in the alloy 316 + Hf (900 °C HT). A coarsening of the precipitate distribution is observed.

microstructure evolution. The dose dependence of number density, size and interstitial volume fraction for Frank loops in alloy 316 + Pt revealed a high loop density, large loop size and loop volume fraction at low doses and a continued decrease of each with doses above 2 dpa. This suggests that Pt addition promote loop nucleation and growth. The subsequent decrease in average loop size is likely caused by the unfaulting of large loops and a reduction in interstitial partitioning to loop growth caused by void competition for interstitials that is more pronounced than in the base 316SS. Void swelling is higher in the alloy 316 + Pt than in the base alloy. The dominant effect of Pt addition on radiation damage is likely the preferential bonding of vacancies with Pt and the enhanced void formation in contrast to the enhanced recombination of point defects in the matrix.

4.2. Influence of Hf

The effect of Hf addition on the irradiated microstructure is more complex than Pt addition. Hafnium is a reactive element and can react with impurities or alloying elements to form various Hf-compounds, such as HfC and $HfNi_5$ intermetallics, thus changing the matrix chemistry. The presence of Hf-rich precipitates and their evolution with dose can affect microstructural development. The misfit for Hf solute addition is much larger than for Pt addition, as indicated in Table 1. The significant improvement of Hf addition on the alloy 316 + Hf (1100 °C HT) suggests an enhanced recombination of point defects. A homogenous distribution of Hf in the matrix is likely a key to maintaining its effectiveness as a trapping site for promoting defect recombination, therefore reducing the formation of radiation damage.

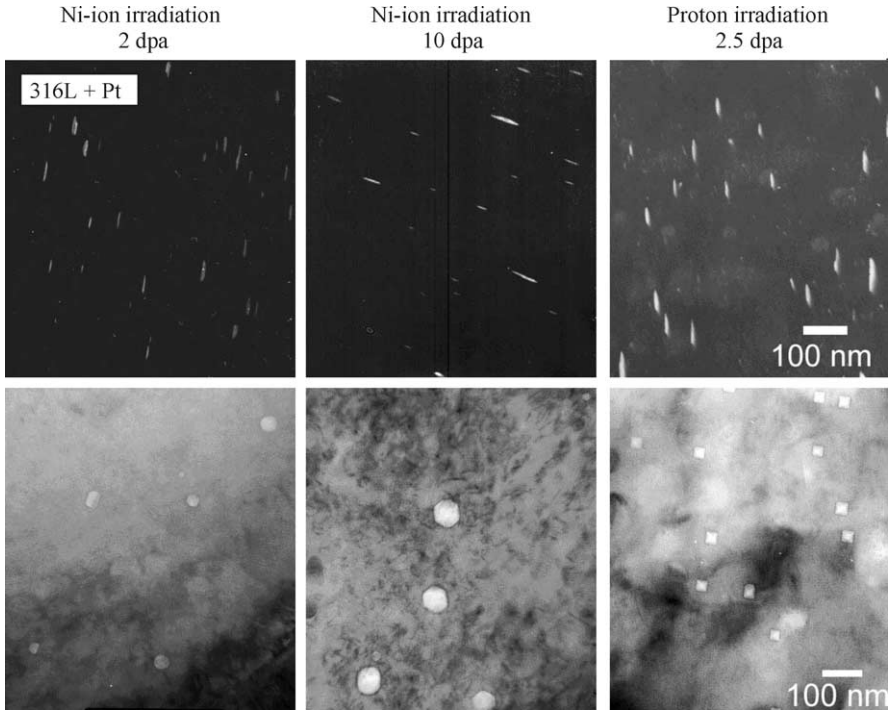

Fig. 12. Comparison of the irradiated microstructure showing Frank loops and voids in alloy 316 + Pt irradiated with Ni^{++} ions at 500 °C and protons at 400 °C at comparable doses.

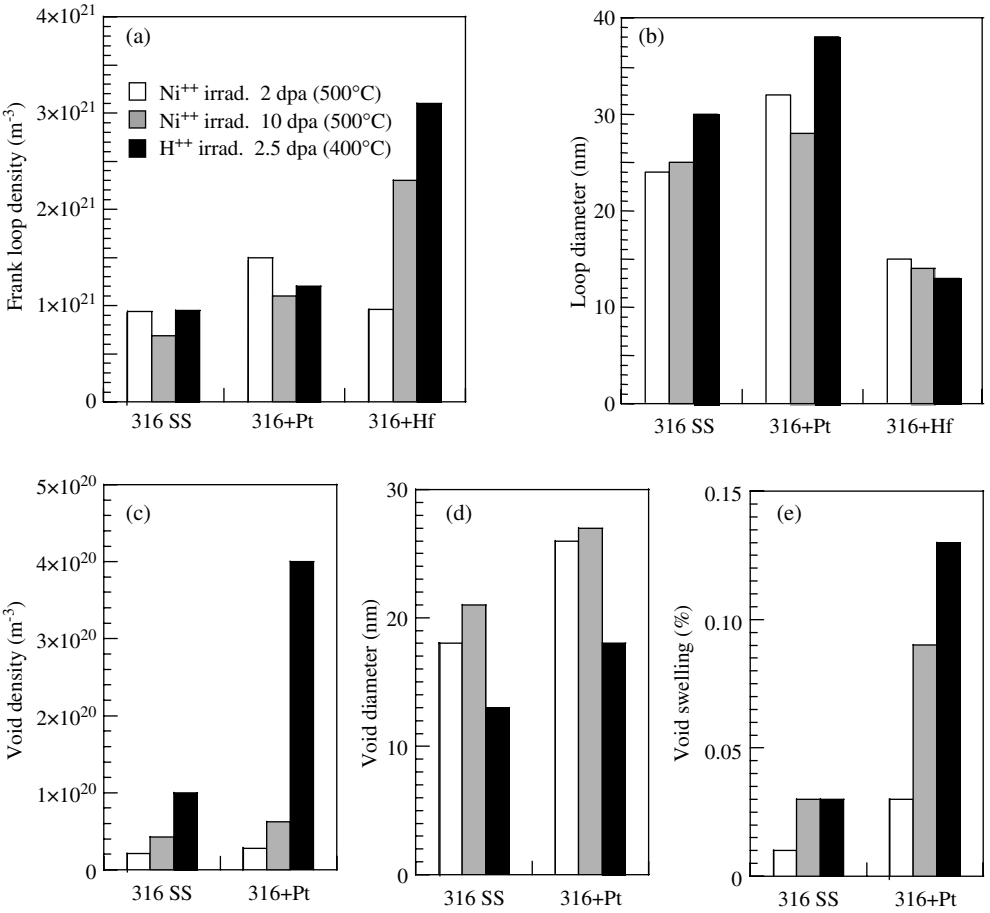

Fig. 13. Comparison of the irradiated microstructure and void swelling between Ni-ion irradiation at 500 °C to doses of 2 and 10 dpa and proton irradiation at 400 °C to a dose 2.5 dpa in alloys 316SS, 316 + Pt and 316 + Hf (1100 °C).

The Hf-doped alloys showed a delayed, but continued increase of loop density and smaller loop sizes with doses up to 50 dpa (more pronounced in 900 °C HT). An initial heat treatment at 1100 °C before irradiation changed the magnitude of loop density and loop volume fraction, but maintained the same trend with increasing dose. The low number density ($<10^{19}$ ppt/m^3) of $HfNi_5$ intermetallics particles in 1100 °C heat-treated alloy along with the scattered and irregular-shaped large HfC inclusions makes an estimation of Hf and C in solution not feasible. It was assumed that the 1100 °C heat treatment put more Hf, C and Ni back in solution than the 900 °C heat-treated alloy, thus point defect recombination was enhanced and loop density was reduced. The Frank loop microstructure in 316 + Hf is not saturated even up to dose of 50 dpa, in contrast to the 316SS and 316 + Pt alloys where loop density is saturated at a dose of 2 dpa. The smaller loop sizes indicate that the Hf addition suppresses loop growth. One possible mechanism is that Hf in solution increases the stress field which increases diffusion barrier for interstitials and promotes mutual annihilation of vacancies and interstitials. This reduces the interstitial partitioning to loop growth and the vacancy partitioning to void nucleation.

No evidence exists to show a local association between voids and precipitates in the microstructure. However since the 1100 °C heat treatment had a stronger impact on void formation, the uniformly distributed $HfNi_5$ precipitates in 900 °C heat-treated 316 + Hf may change the local chemistry and provide a condition favorable for void formation at higher doses. It appears to be important to keep Hf in solution at a reasonable concentration for maintaining the radiation damage resistance. The 1100 °C 316 + Hf alloy in which the precipitate density is dramatically reduced has demonstrated a significant improvement in its resistance to radiation damage, attributing to a higher concentration of Hf solute atoms in the matrix.

4.3. The comparison between Ni^{++} and proton irradiation

Nickel-ion irradiation and proton irradiation have significant differences in cascade morphology. Nickel ions produce point defects mainly in large cascades whereas protons produce damage mainly through wildly separated small cascades, which is a consequence of the bombarding particle mass. If the effect of oversized solute addition on microstructure is mainly within the cascade process, Ni-ion irradiation should show stronger effects than proton irradiation. The agreement between the two different types of irradiation indicates the major effect of the oversized solute addition is not in the cascade process but in the post-cascade defect partitioning to the microstructure evolution. The void density after proton irradiation of 316SS and 316 + Pt alloys is several times higher than after Ni-ion irradiation, shown in Fig. 13(d). This may relate to the dose rate effect on the swelling. The dose rate for the proton irradiation is about two orders of magnitude lower than for Ni-ion irradiation in this work. For the same dose and temperature, swelling is more pronounced at lower dose rates [18–20]. The effect of Pt addition on promoting void nucleation is more obvious in proton irradiation than in Ni-ion irradiation. This is possibly due to that protons are more effective in producing freely migrating point defects. Thus, the point defect interactions with solute addition are more pronounced in proton irradiation.

4.4. Comparison with electron and neutron irradiation

The results from this work are in agreement with electron irradiation at 500 °C on the beneficial effect of Hf addition on suppressing void swelling and RIS at grain boundaries [2]. The comparable irradiation temperature and the high damage rate between Ni-ion and electron irradiation may be important for producing the similar result. This again demonstrates that the effect of oversize solute addition on microstructure is through its impact on the point defect interactions and diffusion, not the cascade process. The result from neutron irradiation at 425 °C to a dose of 35 dpa indicated a beneficial effect from Hf addition [4] revealed by less void swelling than in the alloy 316L. The comparison of Ni-ion results at 500 °C to 50 dpa in the alloy 316 + Hf (1100 °C) with neutron irradiation at 425 °C to 35 dpa is in agreement in that Hf has a beneficial effect on suppressing void swelling. However, it is also in contrast in that no voids were observed for Ni-ion irradiation at 50 dpa but the void microstructure was well developed in neutron irradiation at 35 dpa. Note that although ion irradiations take advantage of the high dose rate and significantly low radioactivity, the use of ion irradiation results should be compared with neutron irradiation results with extra care. Neutron irradiation of the alloys used in this work has been completed in a fast reactor at a temperature of 330 °C relevant to LWR core. The results from Ni-ion and proton irradiation will be combined with the result from neutron irradiation for the same heats and thus provide an opportunity for a full investigation of oversized element effects on radiation damage using three different irradiation particles.

5. Conclusion

The addition of 0.3 at.% Hf solute in 316SS can significantly improve the material resistance to radiation damage by slowing down loop development and suppressing voids up to a dose of 50 dpa in Ni-ion irradiation at 500 °C. The absence of a beneficial effect of Pt addition (10% size misfit) on microstructural evolution is in contrast to the dominant influence of Hf addition (26% size misfit). The size misfit of Hf addition has a much stronger effect over that of Pt addition on the irradiated microstructure. This work reveals that oversize solute additions affect the irradiated microstructure mainly through intra-cascade processes, not in-cascade processes as demonstrated by the consistency between Ni-ion and proton irradiations.

Acknowledgements

The authors are grateful to S. Thevuthasan and V. Shutthanandan for nickel-ion irradiation carried out at Pacific Northwest National Laboratory and V. Rotberg and O. Toader for their help in conducting proton irradiation at the University of Michigan Ion Beam Laboratory. We also thank P.L. Andresen at General Electric Corporate Research & Development for providing the high-purity alloys. The authors acknowledge L.E. Thomas for help on the analysis of the Hf-precipitates. We are grateful to Frank Garner for helpful discussion through out this work. This research was supported by the Office of Nuclear Energy Science and Technology, the Office of Basic Energy Sciences and the Division of Materials Sciences, US Department of Energy, under Contract DE-AC06-76RLO 1830.

References

[1] Y.J. Kim, L.W. Niedrach, P.L. Andresen, Corrosion (USA) 52 (10) (1996) 738.
[2] T. Kato, H. Takahashi, M. Izumiya, Mater. Trans. Jpn. Inst. Met. 32 (1991) 921.
[3] T. Kato, H. Takahashi, M. Izumiya, J. Nucl. Mater. 189 (1992) 167.
[4] S. Ohnuki, S. Yamashita, H. Takahashi, T. Kato, in: M.L. Hamilton, A.A.S. Kumar, S.T. Rosinski, M.L. Grossbeck (Eds.), 19th International Symposium, ASTM STP 1366,

American Society for Testing and Materials, West Conshohocken, PA, 2000.
[5] F.A. Smidt Jr., J.A. Sprague, Scr. Metall. 7 (1973) 495.
[6] F.A. Smidt Jr., J.A. Sprague, Scr. Metall. 7 (1973) 1065.
[7] D.K. Wilsdorf, Scr. Metall. 7 (1973) 1059.
[8] F.A. Garner, in: B.R.T. Frost (Ed.), Nuclear Materials, in: R.W. Cahn, P. Hassen, E.J. Kramer (Eds.), Materials Science and Technology – A Comprehensive Treatment, vol. 10A, 1994, p. 420.
[9] E.P. Simonen, S.M. Bruemmer, J. Nucl. Mater. 239 (1996) 185.
[10] J.I. Cole, S.M. Bruemmer, J. Nucl. Mater. 225 (1995) 53.
[11] J.L. Brimhall, J.I. Cole, J.S. Vetrano, S.M. Bruemmer, in: Proceedings of Microstructure of Irradiated Materials, vol. 373, Materials Research Society, Pittsburgh, PA, 1995, p. 177.
[12] J.M. Cookson, R.D. Carter Jr., D.L. Damcott, M. Atzmon, G.S. Was, J. Nucl. Mater. 202 (1993) 104.
[13] T.R. Allen, G.S. Was, Acta Mater. 46 (1998) 3679.
[14] J. Gan, G.S. Was, J. Nucl. Mater. 297 (2001) 161.
[15] J. Gan, E.P. Simonen, D.J. Edwards, S.M. Bruemmer, L. Fournier, B.H. Sencer, G.S. Was, in: G.E. Lucas, L. Snead, M.A. Kirk Jr., R.G. Elliman (Eds.), Proceedings of MRS Full meeting, 2000, Microstructural Process in Irradiated Materials, vol. 650.
[16] D.L. Damcott, J.M. Cookson, R.D. Carter Jr., J.R. Martin, M. Atzmon, G.S. Was, Radiat. Eff. Def. Solids 118 (1991) 383.
[17] D.B. William, C.B. Carter, Transmission Electron Microscopy, vol. III, Plenum, New York, 1996.
[18] F.A. Garner, M.B. Toloczko, B.H. Sencer, J. Nucl. Mater. 276 (2000) 123.
[19] T. Okita, N. Sekimura, F.A. Garner, L.R. Greenwood, W.G. Wolfer, Y. Isobe, in: 10th International Conference on Environmental Degradation of Materials in Nuclear Power Systems – Water Reactors, 2001, CD-ROM, NACE International, paper No. 91.
[20] F.A. Garner, M.L. Hamilton, B.H. Sencer, T. Okita, N. Sekimura, D.L. Porter, T.R. Allen, W.G. Wolfer, in: Proceedings of ICFRM-10, October 2001, in press.